



Greater Somatosensory Afference With Acupuncture Increases Primary Somatosensory Connectivity and Alleviates Fibromyalgia Pain via Insular γ -Aminobutyric Acid: A Randomized Neuroimaging Trial

Ishtiaq Mawla,¹  Eric Ichesco,¹  Helge J. Zöllner,² Richard A. E. Edden,² Thomas Chenevert,¹ Henry Buchtel,¹ Meagan D. Bretz,¹ Heather Sloan,¹ Chelsea M. Kaplan,¹ Steven E. Harte,¹ George A. Mashour,¹ Daniel J. Clauw,¹ Vitaly Napadow,³ and Richard E. Harris¹

Objective. Acupuncture is a complex multicomponent treatment that has shown promise in the treatment of fibromyalgia (FM). However, clinical trials have shown mixed results, possibly due to heterogeneous methodology and lack of understanding of the underlying mechanism of action. The present study was undertaken to understand the specific contribution of somatosensory afference to improvements in clinical pain, and the specific brain circuits involved.

Methods. Seventy-six patients with FM were randomized to receive either electroacupuncture (EA), with somatosensory afference, or mock laser acupuncture (ML), with no somatosensory afference, twice a week over 8 treatments. Patients with FM in each treatment group were assessed for pain severity levels, measured using Brief Pain Inventory (BPI) scores, and for levels of functional brain network connectivity, assessed using resting state functional magnetic resonance imaging (MRI) and proton magnetic resonance spectroscopy in the right anterior insula, before and after treatment.

Results. Fibromyalgia patients who received EA therapy experienced a greater reduction in pain severity, as measured by the BPI, compared to patients who received ML therapy (mean difference in BPI from pre- to posttreatment was -1.14 in the EA group versus -0.46 in the ML group; P for group \times time interaction = 0.036). Participants receiving EA treatment, as compared to ML treatment, also exhibited resting functional connectivity between the primary somatosensory cortical representation of the leg ($S1_{leg}$; i.e. primary somatosensory subregion activated by EA) and the anterior insula. Increased $S1_{leg}$ –anterior insula connectivity was associated with both reduced levels of pain severity as measured by the BPI ($r = -0.44$, $P = 0.01$) and increased levels of γ -aminobutyric acid (GABA+) in the anterior insula ($r = 0.48$, $P = 0.046$) following EA therapy. Moreover, increased levels of GABA+ in the anterior insula were associated with reduced levels of pain severity as measured by the BPI ($r = -0.59$, $P = 0.01$). Finally, post-EA treatment changes in levels of GABA+ in the anterior insula mediated the relationship between changes in $S1_{leg}$ –anterior insula connectivity and pain severity on the BPI (bootstrap confidence interval -0.533 , -0.037).

Conclusion. The somatosensory component of acupuncture modulates primary somatosensory functional connectivity associated with insular neurochemistry to reduce pain severity in FM.

Supported by the National Institute of Diabetes and Digestive and Kidney Diseases, NIH (grant F99-DK-126121 awarded to Mr. Mawla) and the National Center for Complementary and Integrative Health, NIH (grant R01-AT-007550 awarded to Drs. Napadow and Harris). The present study applied tools developed by the NIH (grants R01-EB-016089 and P41-EB-015909).

¹Ishtiaq Mawla, MS, Eric Ichesco, BS, Thomas Chenevert, PhD, Henry Buchtel, RAc, Meagan D. Bretz, RAc, Heather Sloan, RAc, Chelsea M. Kaplan, PhD, Steven E. Harte, PhD, George A. Mashour, MD, PhD, Daniel J. Clauw, MD, Richard E. Harris, PhD: University of Michigan, Ann Arbor; ²Helge J. Zöllner, PhD, Richard A. E. Edden, PhD: Johns Hopkins University School of Medicine

and Kennedy Krieger Institute, Baltimore, Maryland; ³Vitaly Napadow, PhD: Massachusetts General Hospital, Harvard Medical School, and Brigham and Women's Hospital, Boston, Massachusetts.

Drs. Napadow and Harris contributed equally to this work.

No potential conflicts of interest relevant to this article were reported.

Address correspondence to Richard E. Harris, PhD, 24 Frank Lloyd Wright Drive, Lobby M, Suite 3100, Ann Arbor, MI 48106-5737. Email: reharris@med.umich.edu.

Submitted for publication August 7, 2020; accepted in revised form December 8, 2020.

INTRODUCTION

Fibromyalgia (FM) is a common chronic pain condition affecting 2–8% of the population and is characterized by widespread somatic pain, fatigue, poor sleep, negative mood, and cognitive disturbances (1). While peripheral factors, such as small fiber neuropathy (2) and the immune system (3), may play some role in FM, the disorder is thought to be associated primarily with aberrant physiologic processes in the central nervous system (CNS) which amplifies the perception of pain (also known as “centralized” or “nociplastic” pain [4]). Notably, neuroimaging research has shown that FM patients exhibit increased levels of the excitatory neurotransmitter glutamate (5), decreased levels of the inhibitory neurotransmitter γ -aminobutyric acid (GABA) (6), and up-regulated GABA type A (GABA)_A receptor concentration (7) within the insula. Moreover, increased functional brain network connectivity to pronociceptive areas of the brain and decreased connectivity to antinociceptive areas of the brain have been found in FM (8–10). These results suggest that the CNS is a prime target for therapeutic interventions for FM.

Due to the ongoing opioid public health crisis (11), nonpharmacologic interventions for FM, such as acupuncture, have been gaining attention. However, meta-analyses of acupuncture trials have shown mixed results, with some showing that verum (active) acupuncture is no more effective than sham controls (12,13), whereas other studies have shown that acupuncture is superior to both sham and no-acupuncture controls in reducing pain (14). One reason for the mixed meta-analysis results may be the inclusion of heterogeneous treatment paradigms and sham controls across different trials. Acupuncture is a complex procedure that consists of multiple methodologic components (e.g., needling sensation, location, depth, among others) and contextual components (e.g., expectancy, patient–practitioner rapport, treatment ritual) (15). Importantly, sham controls used in previous acupuncture trials may not have properly accounted for all of these different components of acupuncture.

In the present study, we specifically evaluated CNS mechanisms of action underlying the somatosensory afferent component of acupuncture, and how such mechanisms may prompt an analgesic response in FM. Since verum acupuncture produces somatosensory sensation through needling and palpation, we designed a comparator sham control procedure to lack all aspects of tactile sensation. Many previous trials on acupuncture therapy used sham controls with acupoint palpation and tactile stimulation, mimicking real needle insertion and manipulation, thus confounding verum and sham acupuncture in terms of somatosensory afference (12–14). We randomized FM patients into 2 separate acupuncture therapy groups: electroacupuncture (EA), which has somatosensation, and mock laser acupuncture (ML), which has no somatosensation. EA therapy has been demonstrated to be clinically effective at reducing pain in FM (13). We hypothesized

that EA therapy would specifically recruit somatosensory pathways in the CNS in order to produce greater analgesia compared to ML therapy.

PATIENTS AND METHODS

Study protocol. The present study was designed as a single center, blinded, sham-controlled, randomized non-crossover longitudinal neuroimaging trial, was preregistered with the NIH (ClinicalTrials.gov identifier: NCT02064296), and was carried out at the University of Michigan (Ann Arbor) from December 2014 to November 2019. Study protocols were approved by the University of Michigan Institutional Review Board (IRB) and conducted in accordance with the Declaration of Helsinki. All study participants provided written informed consent.

Study participants and timeline. Individuals with FM were recruited for the study. Full details of inclusion and exclusion criteria are provided in the Supplementary Methods, available on the *Arthritis & Rheumatology* website at <http://onlinelibrary.wiley.com/doi/10.1002/art.41620/abstract>. Following screening, participants were invited to complete a baseline behavioral assessment (day 0) and baseline magnetic resonance imaging (MRI) assessment (occurring sometime between day 1 and day 3), and eligible subjects were randomly assigned to 1 of 2 parallel study arms (Figure 1A) via computer-generated permuted block randomization (blocks of 4, 6, or 8). An acupuncturist was informed of the group allocation of each participant through a sealed envelope, which was not accessible by the principal investigators, study staff, or data analysts. The 2 intervention arms were 1) EA therapy, with somatosensory afference, and 2) ML therapy, without somatosensory afference. After treatment, a second behavioral assessment (performed sometime between days 33 and 40 of the study) and a second MRI assessment (performed sometime between days 34 and 43) were collected. Patient-reported outcomes were collected before and after therapy during the behavioral session. Whole-brain resting state functional MRI (fMRI) and right anterior insula proton magnetic resonance spectroscopy (¹H-MRS) scans were collected during MRI sessions before and after therapy.

Acupuncture treatment. Study participants with FM received 8 treatments with EA or ML twice a week over 4 weeks. During all treatment sessions, participants were positioned supine on an examination table and blindfolded. Blindfolding ensured masking of the treatments in order to avoid any visual afference, as visual afference can also influence acupuncture-induced analgesia (16). All treatments were performed by 3 trained acupuncturists (HB, MDB, and HS) who had board certification from the National Certification Commission for Acupuncture and Oriental Medicine.

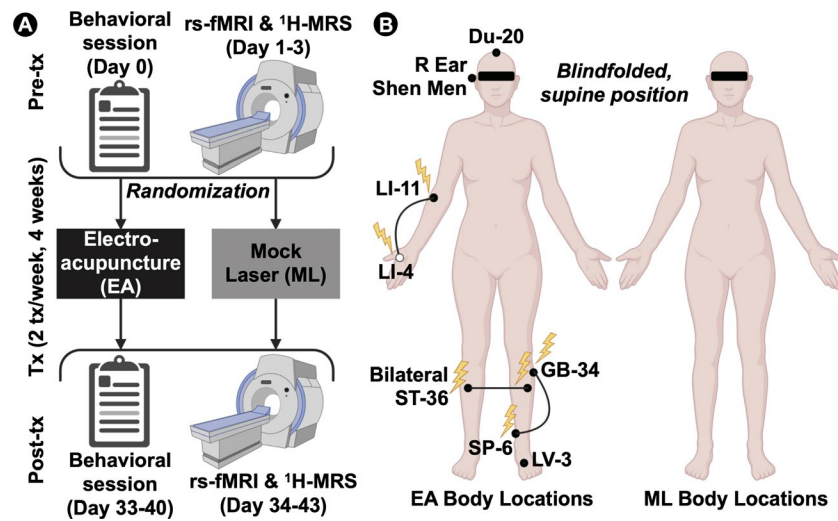


Figure 1. Study overview of non-crossover randomized controlled neuroimaging trial of fibromyalgia (FM) patients with acupuncture intervention. **A**, Behavioral session, resting state functional magnetic resonance imaging (rs-fMRI), and proton magnetic resonance spectroscopy (^1H -MRS) images were collected at baseline (Pre-tx) and posttherapy (Post-tx). **B**, Acupuncture locations for EA and ML treatment. All subjects were blindfolded and placed in a supine position. In the EA group, stimulation was administered to the large intestine 4 (LI-4) acupoint of the dorsal surface of the right (R) hand and to the LI-11 acupoint of the crease of the right elbow. Bolt symbols indicate where needles received current through the EA device. For ML treatment, a deactivated laser was hovered over the same acupuncture points as in the EA group for the same duration of time. Du-20 = Governor meridian; ST-36 = stomach 36; SP-6 = spleen 6; GB-34 = gall bladder 34; LV-3 = liver 3.

The EA group received low-frequency EA at 3 pairs of acupoints: right LI-11 to LI-4 (large intestine 11 to large intestine 4), left GB-34 (gall bladder 34) to SP-6 (spleen 6), and bilateral ST-36 (stomach 36). Needles were also inserted in Du-20 (Governor meridian), right ear Shen Men, and left LV-3 (liver 3) (Figure 1B), but no electrical current was delivered to these sites. EA needles were stimulated with low intensity and frequency using a constant-current electroacupuncture device (AS Super 4 Digital Needle Stimulator), which allowed for flexible setting of pulse width (1 msec), frequency (2 Hz), and shape (biphasic rectangular) parameters. The current intensity was set at each session for each patient individually at the midpoint between sensory and pain thresholds that are based on typical cutoff values used in clinical practice and our previous EA study on patients with chronic pain (17), with stimulation lasting 25 minutes per session. The duration and frequency of treatment are based on common clinical practice and are within the bounds of previous acupuncture trials (18). The selection of acupuncture sites was based on predominant FM symptoms including multisite pain, headache, gastrointestinal pain and dysfunction, disrupted sleep, and chronic fatigue.

For the ML acupuncture therapy group, a laser acupuncture device (VitaLaser 650; Lhasa OMS) was manually positioned approximately 1–2 cm over all of the same acupoints used in the EA treatment group. There was no palpation prior to positioning the device, and there was no physical contact between the device and skin. The laser light was demonstrated to the participants at the first visit to enhance credibility of the intervention; however, the laser was turned off during the actual treatment, thus removing any potential optically induced or thermal sensation, while maintaining

all treatment rituals, as previously described (19,20) (Figure 1B). ML treatments also lasted 25 minutes.

Participants were not informed about a sham or placebo at consent, so all participants were led to believe that both EA and ML are viable treatments for FM. These blinded procedures were preauthorized by the IRB at the start of the study, and all participants were fully debriefed after the final MRI visit.

The verbal instructions used by acupuncturists were standardized across all treatments (Supplementary Methods). After each treatment, the Massachusetts General Hospital Acupuncture Sensation Scale (MASS) (21) was used to evaluate “De Qi” and perceived somatosensory afference. The 13-item questionnaire included sensations such as soreness, aching, deep pressure, and tingling, among others, on a 0–10 scale, with 0 indicating “none” and 10 indicating “unbearable,” and weighted summation of these sensations constituted the MASS Index. This assessment served as a fidelity check to assess whether FM patients consistently reported increased levels of sensation in response to EA therapy compared to ML therapy. In addition, after the first treatment and the last treatment, a Credibility Questionnaire (Supplementary Methods) was administered which assessed the perception of the validity and credibility of the treatments. This ensured that any differences in clinical or neuroimaging outcomes were not due to differences in the perception of credibility among the study participants.

Clinical outcome measures. *Short-Form Brief Pain Inventory (BPI) severity subscale.* The severity subscale of the Short-Form BPI was the primary clinical outcome measure. The BPI severity subscale assesses worst pain in 24 hours,

least pain in 24 hours, pain on average, and pain right now. Pain severity as measured by the BPI was assessed before and after therapy. As a secondary clinical outcome measure, the severity of anxiety and depression was scored using the Patient-Reported Outcomes Measurement Information System (PROMIS) (<https://www.healthmeasures.net/explore-measurement-systems/promis>). The anxiety and depression scores were also used to assess whether neuroimaging outcomes were influenced by these factors. Furthermore, we collected a series of exploratory outcome measures, which included pain interference as measured by the BPI, the American College of Rheumatology 2010 modified criteria for FM (22), pain catastrophizing scores measured using the Pain Catastrophizing Scale (23), and PROMIS scores of physical function, fatigue, and sleep. Descriptive statistics for each exploratory outcome measure are available in the Supplementary Results, available on the *Arthritis & Rheumatology* website at <http://onlinelibrary.wiley.com/doi/10.1002/art.41620/abstract>.

Resting state functional connectivity scans of the primary somatosensory cortex (mechanistic outcome measure). Resting state fMRI scans (performed in study participants while in an eyes-open resting state) and anatomic T1-weighted MRI scans were acquired with a 15-channel head coil in a 3.0T MRI system (Philips Ingenia). Minimal preprocessing of resting state fMRI and T1 images were performed using fMRIPrep version 1.1.8 (24). Full details of the MRI acquisition parameters and preprocessing steps are provided in the Supplementary Methods.

Since somatosensory afferent input is encoded in the primary somatosensory cortex (S1), we chose the S1 cortical representation of the legs as the seed region to examine somatosensory circuits (i.e., communication between S1_{leg} and other brain regions). S1_{leg} was the chosen seed as most EA needles were placed on the leg (Figure 1B), and our group has previously localized this S1_{leg} region in FM patients (centroid Montreal Neurological Institute [MNI] x,y,z coordinates of ±8, -38, 68) (25). Bilateral spherical seeds (4-mm radius) were used to extract fMRI time series, and seed-to-voxel correlation analysis was used to evaluate whole-brain connectivity maps for S1_{leg}. Time series from the S1_{leg} seed (fslmeans) were used as a generalized linear model regressor (fsl_glm) to obtain whole-brain parameter estimates and associated variances for each participant. These parameter estimates and variances were then passed on to group level analysis, conducted on an FMRIB (Oxford Centre for Functional Magnetic Resonance Imaging of the Brain) Local Analysis of Mixed Effects (FLAME 1+2) algorithm (26) to improve mixed-effects variance estimation. S1_{leg} connectivity was then contrasted between pretreatment and post-treatment periods using paired sample *t*-tests for EA and ML therapies separately. Interactive effects between EA and ML therapy were evaluated using an independent samples *t*-test of the paired posttreatment-pretreatment difference images. As age influences neuroimaging outcomes, it was included as a regressor of no interest in all analyses. Multiple comparisons familywise error correction

was conducted using a Gaussian random-field cluster threshold of $Z > 2.3$, and corrected *P* values less than or equal to 0.05 were considered significant.

¹H-MRS measurement of Glx and GABA+ in the right anterior insula (mechanistic outcome measure). ¹H-MRS spectra were acquired from automated voxel placement covering the right anterior insula, as our previous study showed differences between FM and pain-free controls in this region (6). The ¹H-MRS voxel dimensions were based on our previous study (6). Single-voxel point-resolved spectroscopy (PRESS) was used to measure Glx. A separate GABA+-edited Mescher-Garwood-PRESS (MEGA-PRESS), which co-edits signals from macromolecules and homocarnosine, was conducted to estimate GABA+ levels (27). Conventional PRESS spectroscopy data were analyzed with LCModel (28). MEGA-PRESS spectra were processed in Gannet version 3.1.5 (29), a MatLab-based toolbox specifically developed for edited MRS. Full details of PRESS and MEGA-PRESS acquisition parameters, preprocessing, and analysis details are provided in the Supplementary Methods. The final GABA+ estimates are expressed in institutional units (IU), which approximates millimolar concentrations of GABA+, and are also expressed as an integral ratio with respect to the creatine signal (GABA+/Cr). Treatment-related change in Glx and GABA+ was computed as the difference between pretherapy and posttherapy values.

Statistical analysis. Besides the aforementioned image-based statistics, statistical analyses were performed in SPSS software version 26 (IBM). For comparison of changes in the primary clinical outcome measure (pain severity measured by the BPI) and secondary outcome measures (data in the Supplementary Results), an analysis of variance (ANOVA) with 2 × 2 mixed design (assessing groups [EA or ML] by time [pretreatment or posttreatment] interaction) was conducted. An ANOVA with a 2 × 8 mixed design (assessing group [EA or ML] by time [pretreatment or posttreatment] interaction) was used for comparisons of the MASS Index. Geisser-Greenhouse correction was used to adjust for sphericity assumptions in the repeated-measures ANOVA. Mean credibility scores were assessed for group differences using an independent samples *t*-test. Associations between changes in extracted values for S1_{leg} connectivity, GABA levels, and pain severity as measured by the BPI were conducted using Pearson's correlation adjusted for age.

To determine whether relationships assessed with Pearson's correlation coefficient were directionally different for the EA group compared to the ML group, the single-tailed Fisher's *z* cocor algorithm was used (30). For mediation analyses, bias-corrected bootstrapped (×10,000) mediation was conducted using the Process Macro with SPSS software (31), and estimates of indirect effects were computed at the 95% confidence level (adjusted for age).

All charts were created on GraphPad PRISM version 8.2.1 software. Scientific images were created using BioRender.com.

RESULTS

Clinical characteristics and demographics. The flow of study participants in the protocol is described in the Supplementary Results. Full demographic and clinical characteristics and medication usage for each participant are also listed in the Supplementary Results.

Greater posttherapy reduction in pain severity in the EA treatment group compared to the ML treatment group.

For pain severity, as measured by the BPI, results from two-way group \times time mixed-design ANOVA demonstrated a significant main effect of time (degrees of freedom [F] [1, 70] = 25.09, $P < 0.001$) and no main effect of group (F [1, 70] = 0.03, $P = 0.861$). However, there was a significant group \times time interaction (F [1, 70] = 4.56, $P = 0.036$), showing that EA treatment reduced pain severity, as measured by the BPI, to a greater extent compared to ML treatment (Figure 2A). There was no baseline difference in pain severity between the EA and ML treatment groups (t [70] = 0.85, $P = 0.396$). Changes in pain severity were not related to changes in depression (r [33] = 0.24, $P = 0.165$ for the EA group and r [35] = -0.08 , $P = 0.65$ for the ML group) or anxiety (r [33] = 0.07, $P = 0.71$ for the EA group; r [35] = 0.17, $P = 0.31$ for the ML group).

Greater somatosensory afference with EA therapy compared to ML therapy.

For MASS Index scores, the 2×8 (group \times time) mixed-design ANOVA demonstrated a significant main effect of time (F [4.0, 224.9] = 2.85, $P = 0.025$), a significant main effect of group (F [1, 56] = 31.01, $P < 0.001$), but no group \times time interaction effect (F [4.0, 224.9] = 0.35, $P = 0.84$) (Figure 2B). Treatment credibility was equal across both groups (Supplementary Results).

Increased $S1_{leg}$ connectivity posttherapy in the EA treatment group versus the ML treatment group.

A whole-brain seed connectivity analysis of $S1_{leg}$ region showed significant posttherapy increases in connectivity for the EA group, notably to the bilateral anterior insula, posterior insular, and right non-leg $S1$ subregions. Conversely, the ML group showed reductions in $S1_{leg}$ connectivity to the left anterior/mid insula. The whole-brain group \times time interaction effect showed that the magnitude of increase in $S1_{leg}$ connectivity for EA treatment was greater than that of ML treatment, notably showing increased connectivity in regions such as the bilateral anterior insula, posterior insula, and right non-leg $S1$. Relevant contrast images are shown in Figure 3A, and full details of the clusters are available in the Supplementary Results. We also confirmed that resting state fMRI results were not confounded by head motion (Supplementary Results).

Association between increased $S1_{leg}$ connectivity and improvements in pain severity scores in the EA treatment group.

In the EA treatment group, there was a significant relationship between change in $S1_{leg}$ -anterior insula

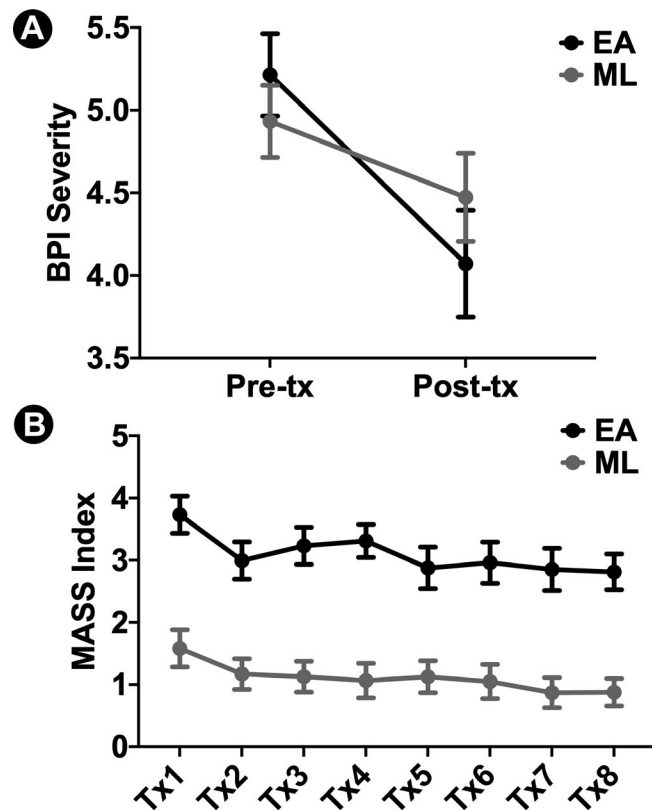


Figure 2. Pain severity on the Brief Pain Inventory (BPI) and Massachusetts General Hospital Acupuncture Sensation Scale (MASS) Index response to acupuncture therapy. **A**, Compared to those who received mock laser acupuncture (ML), fibromyalgia patients who received electroacupuncture (EA) experienced a significantly greater posttherapy (Post-tx) reduction in pain severity as measured by the BPI (P for group \times time interaction = 0.036). **B**, Patients receiving EA therapy reported significantly higher somatosensory afference (MASS Index) compared to those receiving ML therapy ($P < 0.001$ for main effect of group). Bars show the mean \pm SEM.

connectivity and change in pain severity as measured by the BPI (r [30] = -0.44 , $P = 0.01$), such that the greater the increase in $S1_{leg}$ -anterior insula connectivity, the greater the reduction in pain severity, as measured by the BPI, posttherapy (Figure 3B). Change in $S1_{leg}$ -anterior insula connectivity was not related to change in BPI severity in the ML group (r [35] = -0.02 , $P = 0.91$). The correlation between change in $S1_{leg}$ -anterior insula connectivity and change in pain severity scores was significantly stronger in the EA treatment group than in the ML treatment group (Fisher's $z = -1.78$, $P = 0.04$). Changes in $S1_{leg}$ -anterior insula connectivity were not related to posttherapy changes in depression (r [30] = 0.02, $P = 0.93$ in the EA group; r [35] = -0.14 , $P = 0.41$ in the ML group) or anxiety (r [30] = -0.12 , $P = 0.51$ in the EA group; r [35] = 0.11, $P = 0.50$ in the ML group).

Similarly, we found that in the EA treatment group, there was a significant relationship between change in $S1_{leg}$ -posterior insula connectivity and change in pain severity measured by the

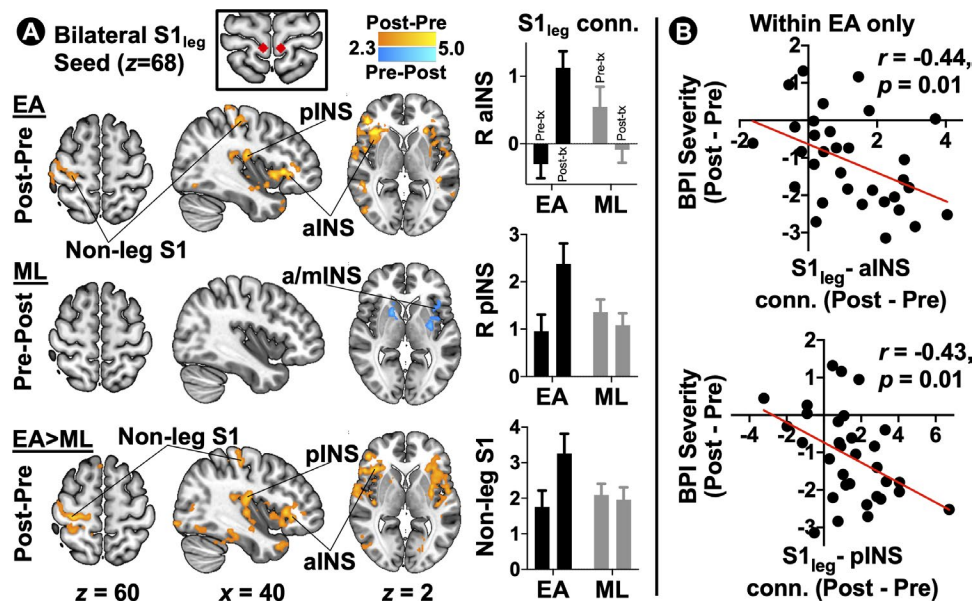


Figure 3. S1_{leg} connectivity (conn.) response to acupuncture stimulation, comparing pretherapy (Pre-tx) and posttherapy (Post-tx) levels of connectivity. **A**, In the electroacupuncture (EA) treatment group, S1_{leg} connectivity to the right anterior insula (R aINS), right posterior insula (R pINS), and non-leg S1 subregion increased with stimulation. In the mock laser acupuncture (ML) treatment group, S1_{leg} connectivity to the anterior insula/mid insula (a/mINS) decreased with stimulation. The EA > ML contrast showed that the magnitude of S1_{leg} connectivity increase was higher in the EA group compared to the ML group. Bars show the mean \pm SEM. **B**, Within the EA treatment group, as S1_{leg}-anterior insula and S1_{leg}-posterior insula connectivity increased, pain severity as measured by the Brief Pain Inventory (BPI) decreased posttherapy. Values have been adjusted for age.

BPI ($r [30] = -0.43, P = 0.01$), such that the greater the increase in S1_{leg}-posterior insula connectivity, the greater the reduction in pain severity posttherapy (Figure 3B). Change in S1_{leg}-posterior insula connectivity was not related to change in pain severity in the ML treatment group ($r [30] = -0.04, P = 0.84$). The correlation between S1_{leg}-posterior insula connectivity and pain severity in the EA treatment group was significantly stronger than that in ML treatment group (Fisher's $z = -1.70, P = 0.04$). Changes in S1_{leg}-posterior insula connectivity were not related to posttherapy

changes in depression ($r [30] = -0.19, P = 0.29$ in the EA group; $r [35] = 0.18, P = 0.29$ in the ML group) or anxiety ($r [30] = -0.24, P = 0.18$ in the EA group; $r [35] = 0.13, P = 0.45$ in the ML group).

Association between changes in anterior insula GABA+ levels and changes in S1_{leg}-anterior insula connectivity in EA treatment. The average MEGA-PRESS spectrum across all subjects is shown in Figure 4A. We found that the right anterior insula cluster from the posttreatment-pretreatment

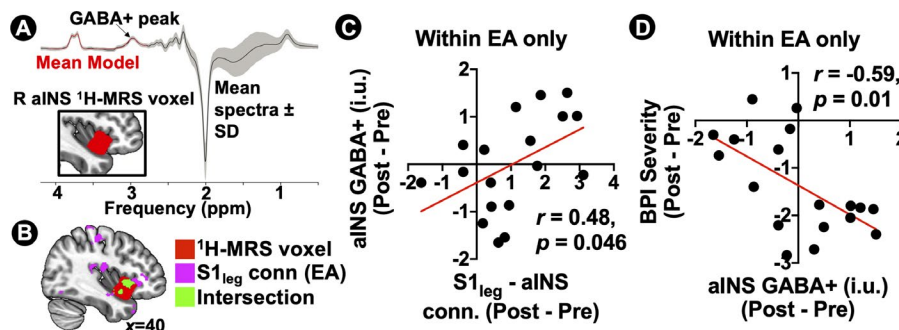


Figure 4. Anterior insula (aINS) γ -aminobutyric acid (GABA) response to electroacupuncture (EA) therapy. **A**, Average spectrum across all subjects of the proton magnetic resonance spectroscopy (¹H-MRS) voxel of the right (R) anterior insula transformed to Montreal Neurological Institute space and the corresponding spectrum frequency in parts per million (ppm) assessed using Mescher-Garwood-single-voxel point-resolved spectroscopy. **B**, Intersection of voxels encompassing both the anterior insula GABA voxel and the anterior insula cluster from the S1_{leg} connectivity (conn.) map. **C**, Greater increase in S1_{leg}-anterior insula connectivity was associated with greater increase in anterior insula GABA+ concentration (measured in institutional units [IU]) posttherapy (Post) relative to pretherapy (Pre). **D**, Greater increase in anterior insula GABA+ was associated with greater reduction in clinical pain, measured using the Brief Pain Inventory (BPI), posttherapy in patients with fibromyalgia. Values have been adjusted for age.

$S1_{leg}$ connectivity group map of the EA therapy group overlapped with the MNI-transformed anterior insula 1H -MRS voxel placement (Figure 4B). There was no main effect of EA or ML treatment on levels of GABA+ (Supplementary Results). However, we found that greater increases in $S1_{leg}$ -anterior insula connectivity were associated with greater increases in GABA+ levels (in IU) in the anterior insula posttherapy (for GABA+ levels, r [16] = 0.48, P = 0.046 [shown in Figure 4C]; for GABA+/Cr, r [16] = 0.46, P for trend = 0.052). This relationship between $S1_{leg}$ -anterior insula connectivity and anterior insula GABA+ levels was not observed in the ML treatment group (for GABA+ levels [in IU], r [23] = -0.17, P = 0.43; for GABA+/Cr, r [23] = -0.15, P = 0.47), and the correlation between $S1_{leg}$ -anterior insula connectivity and anterior insula GABA+ levels was significantly stronger in the EA group than in the ML group (for GABA+ levels [in IU], Fisher's z = 2.08, P = 0.02; for GABA+/Cr, Fisher's z = 1.94, P = 0.03). Furthermore, we confirmed that this relationship was specific to inhibitory, and not excitatory, neurotransmitter changes (Supplementary Results).

Association between changes in anterior insula GABA+ levels and improvements in pain severity as measured by the BPI in the EA treatment group. We found that greater increases in anterior insula GABA+ levels were associated with a greater reduction in BPI pain severity scores (for GABA+ levels [in IU], r [16] = -0.59, P = 0.01 [Figure 4D]; for GABA+/Cr, r [16] = -0.65, P = 0.004). This relationship was not observed in the ML treatment group (for GABA+ levels [in IU], r [16] = -0.16, P = 0.44; for GABA+/Cr, r [23] = -0.13, P = 0.53), and the correlation between increased GABA+ levels in the anterior insula

and reduced pain severity was stronger in the EA group than in the ML group (for GABA+ levels [in IU], Fisher's z = -1.54, P for trend = 0.06; for GABA+/Cr, Fisher's z = -1.92, P = 0.03). Changes in anterior insula GABA+ levels in the EA and ML treatment groups were not related to posttherapy changes in depression (for GABA+ levels [in IU], r [16] = 0.12, P = 0.63 in the EA treatment group and r [23] = 0.07, P = 0.74 in the ML treatment group; for GABA+/Cr, r [16] = 0.23, P = 0.36 in the EA treatment group and r [23] = 0.03, P = 0.89 in the ML treatment group) or anxiety (for GABA+ levels [in IU], r [16] = -0.21, P = 0.40 in the EA treatment group and r [23] = 0.10, P = 0.65 in the ML treatment group; for GABA+/Cr, r [16] = -0.06, P = 0.82 in the EA treatment group and r [23] = 0.08, P = 0.72 in the ML treatment group). Furthermore, we confirmed that this relationship was specific to inhibitory, and not excitatory, neurotransmitter changes (Supplementary Results).

Mediation of the effect of $S1_{leg}$ -anterior insula connectivity on pain severity by anterior insula GABA+ in the EA treatment group. Finally, we conducted a mediation analysis to link $S1_{leg}$ -anterior insula connectivity (X), pain severity as measured by the BPI (Y), and anterior insula GABA+ levels (in IU) (mediator) in one statistical model. Results showed that a greater increase in $S1_{leg}$ -anterior insula connectivity was associated with greater reduction in pain severity posttherapy indirectly through a greater increase in anterior insula GABA+ levels (in IU) (β = -0.187, bootstrapped SE = 0.130, bootstrapped lower limit of the confidence interval = -0.533, bootstrapped upper limit of the confidence interval = -0.037) (Figure 5A). The direct effect of an increase in $S1_{leg}$ -anterior insula connectivity

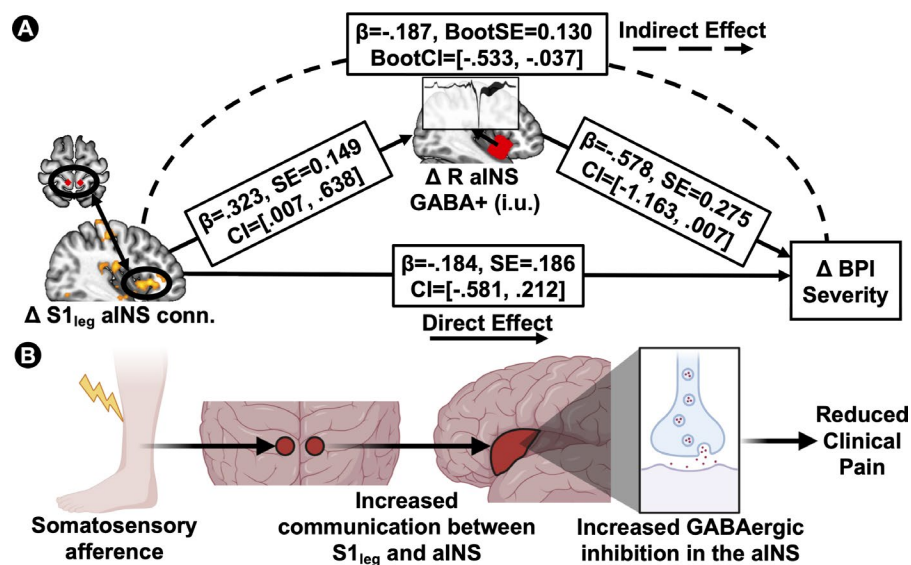


Figure 5. Mediation analysis and proposed mechanistic model. **A**, Increases in levels of γ -aminobutyric acid (GABA)+ (measured in institutional units [IU]) in the right anterior insula (R aINS) mediating the relationship between increased $S1_{leg}$ -anterior insula connectivity (conn.) and decreased pain severity, measured using the Brief Pain Inventory (BPI), posttherapy. **B**, Longitudinally informed mechanistic model proposing that somatosensory afference increases communication between the $S1_{leg}$ subregion and the anterior insula, producing an effect of increased GABAergic inhibition in the anterior insula, leading to reduced clinical pain in patients with fibromyalgia. BootSE = bootstrap SE; BootCI = bootstrap confidence interval.

on the reduction in pain severity posttherapy was not significant (effect = -0.184 , SE = 0.186 , lower limit of the confidence interval = -0.581 , upper limit of the confidence interval = 0.212), suggesting that the effect of S1_{leg}-anterior insula connectivity on pain severity is transmitted through anterior insula GABA+ levels (in IU). The R² value for BPI pain severity in this model was 0.39 . This effect was also present when GABA+/Cr estimates were used as the mediator (Supplementary Results, available on the *Arthritis & Rheumatology* website at <http://onlinelibrary.wiley.com/doi/10.1002/art.41620/abstract>).

DISCUSSION

Our randomized neuroimaging trial evaluated the role of somatosensory afference in acupuncture in the reduction of clinical pain in FM. We found that EA treatment (designed to generate sustained somatosensory afferent activity) was more effective than ML acupuncture (designed to generate no somatosensory afference) in reducing clinical pain. As the EA intervention was heavily directed toward the patient's legs, we examined brain connectivity with the primary somatosensory cortical representation of the leg (S1_{leg}). We found that following EA therapy, increased communication of this S1_{leg} region with the anterior and posterior insula in FM patients was demonstrated, as well as non-leg S1 subregions. Greater posttherapy increases in S1_{leg}-anterior insula and S1_{leg}-posterior insula connectivity were associated with greater reduction in clinical pain. Moreover, we measured the concentration of the inhibitory neurotransmitter GABA in the insula and found that a greater posttherapy increase in S1_{leg}-anterior insula connectivity was associated with a greater increase in anterior insula GABA+, suggesting that S1_{leg} signaling may increase GABAergic inhibition in the anterior insula. Furthermore, we found that greater increases in anterior insula GABA+ were associated with a greater reduction in clinical pain. Finally, increased anterior insula GABA+ mediated the effect of increased S1_{leg}-anterior insula connectivity on reduced clinical pain in EA treatment. Cumulatively, these results allow us to establish a mechanistic model for the role of somatic sensation in acupuncture therapy: somatosensory afference leads to increased S1_{leg}-anterior insula signaling, resulting in increased GABAergic inhibition in the anterior insula, ultimately reducing clinical pain (Figure 5B).

Our research extends previous work demonstrating somatotopically specific involvement of the S1 subregion in acupuncture. Early research in this field of study showed that EA applied to the ST-36 acupoint produced stimulus-evoked blood oxygenation level-dependent (BOLD) activation in the contralateral S1_{leg} region (32). Later work examined somatotopic specificity of S1 morphology and functional involvement in clinical populations, linking S1 metrics with therapeutic outcomes. Specifically, in carpal tunnel syndrome, longitudinal EA therapy targeting the median nerve at the wrist increased the S1 separation distance between median nerve innervated digits 2 and 3, and this increase in S1 digit separation

predicted long-term clinical improvements (17). Another recent study that investigated the use of manual acupuncture in treating chronic low back pain showed increases in gray matter volume and white matter integrity in the back-specific S1 subregion (20). However, these studies were limited to local changes within the S1 region and did not explore cross-network signaling.

There is some evidence of increased cross-network communication in response to acute EA stimulation. In healthy individuals, acute EA stimulation produced increased connectivity of the "Default Mode" and sensorimotor network to the anterior cingulate (a key node of the salience network) (33). In the present study, we found evidence for increased connectivity between the S1_{leg} subregion and right anterior insula, and the degree of this connectivity increase was linked to improvements in clinical pain. This result may seem counterintuitive as chronic nociplastic pain is often characterized by heightened resting functional connectivity of S1 and the anterior insula relative to pain-free controls (34,35). However, those studies assessed pathologic-specific S1 subregions (e.g., S1_{back} for lower back pain). In our study, we evaluated connectivity of S1 subregions specifically targeted by EA therapy (i.e., S1_{leg}). Furthermore, recent work has causally shown that GABAergic inhibition is recruited in the anterior insula to reduce nocifensive behavior (36). Therefore, our results suggest that S1_{leg} may be signaling the anterior insula to reduce clinical pain via GABAergic inhibition. Alternately, acupuncture may temporarily up-regulate pronociceptive signaling between the S1_{leg} subregion and the anterior insula, which may trigger endogenous descending inhibitory systems to counteract through GABAergic inhibition of the anterior insula (i.e., healing processes initiated by temporary injury) (37). These frameworks need further validation through reverse translational studies.

In patients with FM, reduced levels of GABA in the anterior insula (6), and a compensatory up-regulation of GABA type A receptors, have been reported (7). Pharmacologic interventions that enhance GABAergic neurotransmission have been found efficacious for FM, as observed in a phase III randomized trial of sodium oxybate (a GABA agonist) that showed improvements in FM symptoms (38). Based on these observations, reverse translational research has shown a causal link between anterior insula GABA levels and nocifensive behaviors in rats, with decreasing endogenous levels of GABA in the agranular insula (rat homolog of the anterior insula) and increased thermal and mechanical sensitivity (39). Our study extends this literature by showing that increases in anterior insula GABA+ were associated with improvements in clinical pain following EA treatment, suggesting that somatosensory afference may modulate GABAergic inhibition to produce analgesia. The anterior insula is a hyperreactive locus in FM patients (40), and patients who have a posttherapy increase in anterior insula GABA+ levels may experience a reduction in hyperreactivity or hyperactivity in the anterior insula, resulting in analgesia. Interestingly, although GABA is a molecular product of glutamate, our study did not show any association between

clinical outcomes and Glx, suggesting that specific GABAergic pathways may be involved in somatosensation-enhanced acupuncture analgesia.

Another notable link established in our study was that increased long-range cortico–cortico communication posttherapy may lead to increased GABAergic inhibition. Although GABAergic neurons contribute significantly to local energy consumption (41), the relationship between BOLD activity and GABA derived from ¹H-MRS is complex. Some studies in healthy individuals have shown that greater levels of GABA are related to greater task-based negative BOLD responses (42,43) whereas other research across multiple cortical regions has shown no such relationships (44). With regard to BOLD functional connectivity, both positive and negative correlations with GABA have been noted, with greater within-primary motor (M1) connectivity having been shown to be negatively correlated with M1 GABA (45), and whereas dorsal anterior cingulate GABA was not related to salience network GABA (46). One recent study in healthy individuals measured GABA in two nodes of traditionally anti-correlated networks, the medial prefrontal cortex (mPFC) and the dorsolateral prefrontal cortex (dlPFC), and showed that mPFC–dlPFC functional connectivity at rest was positively correlated with dlPFC GABA levels and negatively correlated with mPFC GABA levels (47), suggesting that intrinsic functional connectivity architecture may be associated with varying GABAergic tone across the cortex.

Few studies have noted treatment-related changes in GABA and functional connectivity. It was found in one study that administration of Gamma-hydroxybutyrate (a GABA agonist) increased right anterior insula functional connectivity (48). Due to the complex relationship between GABA and BOLD functional connectivity demonstrated across previous studies, our results need further validation. Nevertheless, our longitudinally informed model (Figure 5B) proposes that increased S1_{leg}–anterior insula connectivity influenced GABA+ in the anterior insula to reduce clinical pain. The downstream effects of this S1_{leg}–anterior insula pathway need further investigation. One possibility is that S1 taps into anterior insula regulation of sympathetic outflow, as the anterior insula is part of the central autonomic network (49). In fact, our previous study has shown that during experimental pressure pain in FM patients, S1_{leg}–anterior insula connectivity was associated with reduced cardiovagal modulation (25). Additionally, GABA is not the only neurotransmitter regulating anterior insula function. In a subsample of FM participants from this study, we found that elevated levels of choline (often involved in neuroinflammation) in FM was related to pain interference via anterior insula–putamen functional connectivity (50). Future studies should more explicitly examine the role of the autonomic nervous system and/or other neurotransmitters involved in somatosensation-induced acupuncture analgesia.

While our study demonstrates mechanistic links of acupuncture treatment via S1_{leg}–anterior insula connectivity and anterior insula GABA levels, the clinical translation of these brain markers

warrants further evaluation. For instance, a possible hypothesis is that anterior insula GABA levels and S1_{leg}–anterior insula connectivity at baseline is predictive of the therapeutic trajectory of acupuncture, which would increase its clinical utility. Future studies should be focused on using neuroimaging markers at baseline to predict acupuncture treatment outcomes.

Our study was designed to specifically examine somatosensory afference, but other contextual factors (patient–clinician rapport, expectations, among others) may have contributed to analgesia as well, particularly in the ML comparator group. Thus, our results highlight the importance of carefully designed controls in acupuncture trials, as various specific and nonspecific components contribute toward treatment outcomes. Researchers need a thorough understanding of the various factors that might be contributing to analgesia while designing an acupuncture trial.

Our study had some limitations. Despite a strong relationship between changes in anterior insula GABA+ levels and changes in clinical pain/S1_{leg}–anterior insula connectivity, we did not observe a main effect of posttherapy GABA+ increase. We reason that the anterior insula may be downstream of our proposed pathway (Figure 5B) and 4 weeks of treatment may not be sufficient to increase GABA+ levels in the anterior insula. Future studies should be designed with a longer treatment schedule, including a post-therapy assessment period to examine long-term effects.

In summary, our study found that the somatosensory component of acupuncture specifically modulated functional communication and inhibitory neurochemistry in the somatosensory–insular circuit in order to reduce clinical pain in FM patients. With future rigorous mechanistic studies of acupuncture, we may be able to discover novel CNS pathways involved in nonpharmacologically induced analgesia and design new treatments that modulate CNS pathways in the pathologic processes leading to chronic pain.

AUTHOR CONTRIBUTIONS

All authors were involved in drafting the article or revising it critically for important intellectual content, and all authors approved the final version to be published. Mr. Mawla had full access to all the study data and takes responsibility for the integrity of the data and the accuracy of the data analysis.

Study conception and design. Mawla, Ichescio, Chenevert, Harte, Mashour, Clauw, Napadow, Harris.

Acquisition of data. Ichescio, Chenevert, Buchtel, Bretz, Sloan.

Analysis and/or interpretation of data. Mawla, Ichescio, Zöllner, Edden, Kaplan, Harte, Mashour, Clauw, Napadow, Harris.

REFERENCES

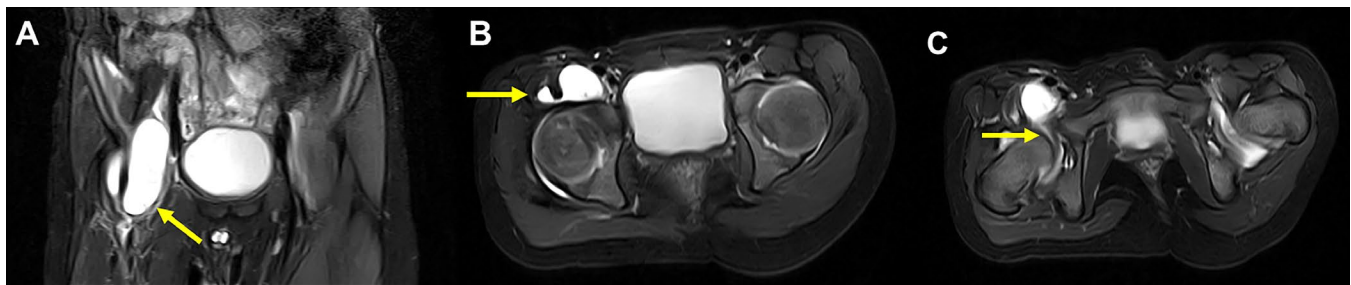
1. Clauw DJ. Fibromyalgia: a clinical review. *JAMA* 2014;311:1547–55.
2. Harte SE, Clauw DJ, Hayes JM, Feldman EL, St. Charles IC, Watson CJ. Reduced intraepidermal nerve fiber density after a sustained increase in insular glutamate: a proof-of-concept study examining the pathogenesis of small fiber pathology in fibromyalgia. *Pain Rep* 2017;2:e590.
3. Kaplan CM, Schrepf A, Ichescio E, Larkin T, Harte SE, Harris RE, et al. Association of inflammation with pronociceptive brain connections in

- rheumatoid arthritis patients with concomitant fibromyalgia. *Arthritis Rheumatol* 2020;72:41–6.
4. Kosek E, Cohen M, Baron R, Gebhart GF, Mico JA, Rice AS, et al. Do we need a third mechanistic descriptor for chronic pain states? *Pain* 2016;157:1382–6.
 5. Harris RE, Sundgren PC, Craig AD, Kirshenbaum E, Sen A, Napadow V, et al. Elevated insular glutamate in fibromyalgia is associated with experimental pain. *Arthritis Rheum* 2009;60:3146–52.
 6. Foerster BR, Petrou M, Edden RA, Sundgren PC, Schmidt-Wilcke T, Lowe SE, et al. Reduced insular γ -aminobutyric acid in fibromyalgia. *Arthritis Rheum* 2012;64:579–83.
 7. Pomares FB, Roy S, Funck T, Feier NA, Thiel A, Fitzcharles MA, et al. Upregulation of cortical GABAA receptor concentration in fibromyalgia. *Pain* 2020;161:74–82.
 8. Napadow V, LaCount L, Park K, As-Sanie S, Clauw DJ, Harris RE. Intrinsic brain connectivity in fibromyalgia is associated with chronic pain intensity. *Arthritis Rheum* 2010;62:2545–55.
 9. Ichesco E, Schmidt-Wilcke T, Bhavsar R, Clauw DJ, Peltier SJ, Kim J, et al. Altered resting state connectivity of the insular cortex in individuals with fibromyalgia. *J Pain* 2014;15:815–26.
 10. Harper DE, Ichesco E, Schrepf A, Hampson JP, Clauw DJ, Schmidt-Wilcke T, et al. Resting functional connectivity of the periaqueductal gray is associated with normal inhibition and pathological facilitation in conditioned pain modulation. *J Pain* 2018;19:635.
 11. Rummans TA, Burton MC, Dawson NL. How good intentions contributed to bad outcomes: the opioid crisis. *Mayo Clin Proc* 2018;93:344–50.
 12. Madsen MV, Gotzsche PC, Hrobjartsson A. Acupuncture treatment for pain: systematic review of randomised clinical trials with acupuncture, placebo acupuncture, and no acupuncture groups. *BMJ* 2009;338:a3115.
 13. Langhorst J, Klose P, Musial F, Irnich D, Hauser W. Efficacy of acupuncture in fibromyalgia syndrome: a systematic review with a meta-analysis of controlled clinical trials. *Rheumatology (Oxford)* 2010;49:778–88.
 14. Vickers AJ, Cronin AM, Maschino AC, Lewith G, MacPherson H, Foster NE, et al. Acupuncture for chronic pain: individual patient data meta-analysis [review]. *Arch Intern Med* 2012;172:1444–53.
 15. Langevin HM, Wayne PM, Macpherson H, Schnyer R, Milley RM, Napadow V, et al. Paradoxes in acupuncture research: strategies for moving forward. *Evid Based Complement Alternat Med* 2011;2011:180805.
 16. Makary MM, Lee J, Lee E, Eun S, Kim J, Jahng GH, et al. Phantom acupuncture induces placebo credibility and vicarious sensations: a parallel fMRI study of low back pain patients. *Sci Rep* 2018;8:930.
 17. Maeda Y, Kim H, Kettner N, Kim J, Cina S, Malatesta C, et al. Rewiring the primary somatosensory cortex in carpal tunnel syndrome with acupuncture. *Brain* 2017;140:914–27.
 18. MacPherson H, Maschino AC, Lewith G, Foster NE, Witt CM, Vickers AJ, et al. Characteristics of acupuncture treatment associated with outcome: an individual patient meta-analysis of 17,922 patients with chronic pain in randomised controlled trials. *PLoS One* 2013;8:e77438.
 19. Irnich D, Salih N, Offenbacher M, Fleckenstein J. Is sham laser a valid control for acupuncture trials? *Evid Based Complement Alternat Med* 2011;2011:485945.
 20. Kim H, Mawla I, Lee J, Gerber J, Walker K, Kim J, et al. Reduced tactile acuity in chronic low back pain is linked with structural neuroplasticity in primary somatosensory cortex and is modulated by acupuncture therapy. *Neuroimage* 2020;217:116899.
 21. Kong J, Gollub R, Huang T, Polich G, Napadow V, Hui K, et al. Acupuncture de qi, from qualitative history to quantitative measurement. *J Altern Complement Med* 2007;13:1059–70.
 22. Wolfe F, Clauw DJ, Fitzcharles MA, Goldenberg DL, Häuser W, Katz RS, et al. Fibromyalgia criteria and severity scales for clinical and epidemiological studies: a modification of the ACR Preliminary Diagnostic Criteria for Fibromyalgia. *J Rheumatol* 2011;38:1113–22.
 23. Sullivan MJ, Bishop SR, Pivik J. The Pain Catastrophizing Scale: development and validation. *Psychol Assess* 1995;7:524–32.
 24. Esteban O, Markiewicz CJ, Blair RW, Moodie CA, Isik AI, Erramuzpe A, et al. fMRIPrep: a robust preprocessing pipeline for functional MRI. *Nat Methods* 2019;16:111–6.
 25. Kim J, Loggia ML, Cahalan CM, Harris RE, Beissner F, Garcia RG, et al. The somatosensory link in fibromyalgia: functional connectivity of the primary somatosensory cortex is altered by sustained pain and is associated with clinical/autonomic dysfunction. *Arthritis Rheumatol* 2015;67:1395–405.
 26. Woolrich MW, Behrens TE, Beckmann CF, Jenkinson M, Smith SM. Multilevel linear modelling for fMRI group analysis using Bayesian inference. *Neuroimage* 2004;21:1732–47.
 27. Mescher M, Merkle H, Kirsch J, Garwood M, Gruetter R. Simultaneous in vivo spectral editing and water suppression. *NMR Biomed* 1998;11:266–72.
 28. Provencher SW. Automatic quantitation of localized in vivo ^1H spectra with LCModel. *NMR Biomed* 2001;14:260–4.
 29. Edden RA, Puts NA, Harris AD, Barker PB, Evans CJ. Gannet: a batch-processing tool for the quantitative analysis of γ -aminobutyric acid-edited MR spectroscopy spectra. *J Magn Reson Imaging* 2014;40:1445–52.
 30. Diedenhofen B, Musch J. Cocor: a comprehensive solution for the statistical comparison of correlations. *PLoS One* 2015;10:e0121945.
 31. Hayes AF. Introduction to mediation, moderation, and conditional process analysis: a regression-based approach. 2nd ed. New York: Guilford; 2017.
 32. Napadow V, Makris N, Liu J, Kettner NW, Kwong KK, Hui KK. Effects of electroacupuncture versus manual acupuncture on the human brain as measured by fMRI. *Hum Brain Mapp* 2005;24:193–205.
 33. Dhond RP, Yeh C, Park K, Kettner N, Napadow V. Acupuncture modulates resting state connectivity in default and sensorimotor brain networks. *Pain* 2008;136:407–18.
 34. Kutch JJ, Ichesco E, Hampson JP, Labus JS, Farmer MA, Martucci KT, et al. Brain signature and functional impact of centralized pain: a multidisciplinary approach to the study of chronic pelvic pain (MAPP) network study. *Pain* 2017;158:1979–91.
 35. Kim J, Mawla I, Kong J, Lee J, Gerber J, Ortiz A, et al. Somatotopically specific primary somatosensory connectivity to salience and default mode networks encodes clinical pain. *Pain* 2019;160:1594–605.
 36. Gamal-Eltrabily M, de Los Monteros-Zuniga AE, Manzano-Garcia A, Martinez-Lorenzana G, Condes-Lara M, Gonzalez-Hernandez A. The rostral agranular insular cortex, a new site of oxytocin to induce antinociception. *J Neurosci* 2020;40:5669–80.
 37. Zhu H. Acupoints initiate the healing process. *Med Acupunct* 2014;26:264–70.
 38. Russell IJ, Holman AJ, Swick TJ, Alvarez-Horine S, Wang YG, Guinta D, et al. Sodium oxybate reduces pain, fatigue, and sleep disturbance and improves functionality in fibromyalgia: results from a 14-week, randomized, double-blind, placebo-controlled study. *Pain* 2011;152:1007–17.
 39. Watson CJ. Insular balance of glutamatergic and GABAergic signaling modulates pain processing. *Pain* 2016;157:2194–207.
 40. Harte SE, Ichesco E, Hampson JP, Peltier SJ, Schmidt-Wilcke T, Clauw DJ, et al. Pharmacologic attenuation of cross-modal sensory augmentation within the chronic pain insula. *Pain* 2016;157:1933–45.
 41. Buzsaki G, Kaila K, Raichle M. Inhibition and brain work. *Neuron* 2007;56:771–83.
 42. Northoff G, Walter M, Schulte RF, Beck J, Dydak U, Henning A, et al. GABA concentrations in the human anterior cingulate cortex predict negative BOLD responses in fMRI. *Nat Neurosci* 2007;10:1515–7.

43. Muthukumaraswamy SD, Edden RA, Jones DK, Swettenham JB, Singh KD. Resting GABA concentration predicts peak γ frequency and fMRI amplitude in response to visual stimulation in humans. *Proc Natl Acad Sci U S A* 2009;106:8356–61.
44. Harris AD, Puts NA, Anderson BA, Yantis S, Pekar JJ, Barker PB, et al. Multi-regional investigation of the relationship between functional MRI blood oxygenation level dependent (BOLD) activation and GABA concentration. *PLoS One* 2015;10:e0117531.
45. Stagg CJ, Bachtiar V, Amadi U, Gudberg CA, Ilie AS, Sampaio-Baptista C, et al. Local GABA concentration is related to network-level resting functional connectivity. *Elife* 2014;3:e01465.
46. Levar N, van Doesum TJ, Denys D, Van Wingen GA. Anterior cingulate GABA and glutamate concentrations are associated with resting-state network connectivity. *Sci Rep* 2019;9:2116.
47. Chen X, Fan X, Hu Y, Zuo C, Whitfield-Gabrieli W, Holt D, et al. Regional GABA concentrations modulate inter-network resting-state functional connectivity. *Cereb Cortex* 2019;29:1607–18.
48. Bosch OG, Esposito F, Dornbierer D, von Rotz R, Kraehenmann R, Staempfli P, et al. Prohedonic properties of γ -hydroxybutyrate are associated with changes in limbic resting-state functional connectivity. *Hum Psychopharmacol* 2018;33:e2679.
49. Beissner F, Meissner K, Bar KJ, Napadow V. The autonomic brain: an activation likelihood estimation meta-analysis for central processing of autonomic function. *J Neurosci* 2013;33:10503–11.
50. Jung C, Ichesco E, Ratai EM, Gonzalez RG, Burdo T, Loggia ML, et al. Magnetic resonance imaging of neuroinflammation in chronic pain: a role for astrogliosis? *Pain* 2020;161:1555–64.


DOI 10.1002/art.41692

Clinical images: Giant iliopsoas bursitis in systemic juvenile idiopathic arthritis



The patient, a 4-year-old boy with systemic juvenile idiopathic arthritis (JIA), experienced a relapse while being treated with tacrolimus and tocilizumab (TCZ), and presented with right groin pain and claudication. Physical examination demonstrated mild tenderness and restricted range of motion in the right hip joint with no palpable mass. Laboratory testing revealed a highly elevated serum matrix metalloproteinase 3 (MMP-3) level (551 ng/dl); however, leukocytosis and C-reactive protein (CRP) elevation (8,700/ μ l and 0.02 mg/dl, respectively) were not observed. Unexpectedly, magnetic resonance imaging demonstrated a giant cyst anterior to the right hip joint and posterior to the iliopsoas muscle (arrows in **A** and **B**). The cyst appeared to be connected to the right hip joint (arrow in **C**). Percutaneous cyst aspiration yielded yellow turbid fluid with leukocytes (58,200/ μ l), predominantly with neutrophils. No bacterial organisms were detected on culture. Iliopsoas (or iliopsoas) bursitis associated with the relapse of systemic JIA was diagnosed. After treatment was switched from TCZ to canakinumab, the patient's symptoms rapidly improved and one month later serum MMP-3 level had returned to normal. Iliopsoas bursitis is a rare condition that has been reported to occur in the setting of various hip diseases including rheumatoid arthritis and traumatic or degenerative conditions, and post-hip replacement (1). Communication between iliopsoas bursa and the hip joint is present in ~14% of the general population and can result from chronic inflammation of the hip joint (2,3). In our patient, it was considered that active synovitis caused a marked increase of the fluid in the hip joint, decompressed into the bursa, and resulted in giant iliopsoas bursitis. TCZ can mask the signs of inflammation, such as fever, pain, local warmth, and CRP elevation. Although iliopsoas bursa is rare, it should be considered in children with systemic JIA presenting with groin pain, particularly those being treated with TCZ even with mild symptoms.

1. Iwata T, Nozawa S, Ohashi M, Sakai H, Shimizu K. Giant iliopsoas bursitis presenting as neuropathy and severe edema of the lower limb: case illustration and review of the literature. *Clin Rheumatol* 2013;32:721–5.
2. Chandler SB. The iliopsoas bursa in man. *Anat Rec* 1934;58:235–40.
3. Sartoris DJ, Danzig L, Gilula L, Greenway G, Resnick D. Synovial cysts of the hip joint and iliopsoas bursitis: a spectrum of imaging abnormalities. *Skeletal Radiol* 1985;14:85–94.

Asami Shimbo, MD
 Yuko Akutsu, MD
 Susumu Yamazaki, MD, PhD
 Masaki Shimizu, MD, PhD 
 Masaaki Mori, MD, PhD
 Tokyo Medical and Dental University
 Tokyo, Japan